AAPS PharmSciTech, Vol. 17, No. 6, December 2016 (© 2016)
DOI: 10.1208/s12249-016-0480-8

Research Article

Development of Molecularly Imprinted Olanzapine Nano-particles: *In Vitro* Characterization and *In Vivo* Evaluation

Nersi Jafary Omid,[1] Hoda Morovati,[1] Mohsen Amini,[2] Ahmad-Reza Dehpour,[3] Alireza Partoazar,[3] Morteza Rafiee-Tehrani,[1] and Farid Dorkoosh[1,4,5]

Received 27 September 2015; accepted 9 January 2016; published online 2 February 2016

Abstract. Molecularly imprinted nano-particles (MINPs) selective for olanzapine were prepared using methacrylic acid (MA) as monomer, ethylene glycol dimethacrylate (EGDMA) as a cross-linker, and 2,2-azobis (2-isobutyronitrile) (AIBN) as the initiator in 36 different ratios. The reaction runs with considerable fine powder formation were selected for further binding and selectivity studies. The MINP with the best selectivity (MINP-32) was chosen for further structural characterization by Fourier transform infrared spectroscopy (FT-IR), thermal gravimetric analysis (TGA), scanning electron microscopy (SEM), adsorption-desorption isotherm for specific surface area, volume and average pore diameter determination. All characterization methods confirmed the successful formation of MINP. The optimum conditions for maximum template loading on the MINP-32 were found by experimental design using response surface methodology (RSM) and choosing absorbent amount, pH, and time as the main factors. MINPs with maximum template loading also indicated significant selectivity between template and its analog (clozapine). The release profile demonstrated a maximum release of about 95% after 288 h for MINP-32 in comparison with about 94% after 120 h for non-MINP-32. The same slow release of drug from MINP-32 was also observed during animal study of the plasma level of template, 20–28 μg/ml *versus* 5–10 μg/ml. The MINP-32 of this study represents a desirable ability to keep the memory of the template with significant selectivity and good capability to control the release of template *in vitro* and *in vivo* and hence could be a promising drug delivery system.

KEYWORDS: experimental design; molecularly imprinted polymers; nano-particles; olanzapine; schizophrenia.

INTRODUCTION

Synthetic polymers are one of the most important materials with diverse properties and application in many aspects of human daily life. Due to technological improvement and thanks to merging in pharmaceutical sciences during the recent 30 years, polymers have found a wide range of applications in this field with functions that encompass simple tasks such as solubilizer, stabilizer, tablet film coater and binder to more complicated ones such as drug release modulation, drug targeting and responsiveness to environmental stimuli as smart polymers (1–3). Polymers in drug delivery perform their function either by governing time control or location control (4).

Molecularly imprinted polymers (MIPs), among other polymers, have been considered in pharmaceutical technology and became attractive due to their unique characteristics. They are polymeric networks which have memorized the configuration of a host molecule known as template. Molecular imprinting is not a new know-how and its technology originated 70–80 years ago but has changed and improved significantly during this period (5). At the beginning, these polymers were applied in different chemical purification and analytical separation techniques and processes (6–8), as scavenger for undesired compounds in food industries (9), as a tool for drug discovery (10), and as enzyme-like catalysts (11). Recently, MIPs are considered as a drug delivery tool as not only they can have better control on drug release in comparison to conventional polymers due to their selective affinity to the host molecule but also they can achieve responsiveness to environmental conditions by employing responsive comonomers in their structure and hence regulate the drug release from the polymeric network (12). MIPs can even be applied in conventional dosage forms such as tablets to modulate the drug release in response to a biomarker (13).

[1] Department of Pharmaceutics, Faculty of Pharmacy, Tehran University of Medical Sciences, Tehran, Iran.
[2] Department of Medicinal Chemistry, Faculty of Pharmacy, Tehran University of Medical Sciences, Tehran, Iran.
[3] Department of Pharmacology, Faculty of Medicine, Tehran University of Medical Sciences, Tehran, Iran.
[4] Pharmaceutical Products Technology Units Incubator, No. 1462, Kargar Ave., Tehran, Iran1439804448.
[5] To whom correspondence should be addressed. (e-mail: dorkoosh@tums.ac.ir)

One of the main features of MIPs is the ease of synthesis. Generally, a template is mixed with one or more functional monomers to make a primary complex which will then be cross-linked by a suitable cross-linker. Different strategies are used to prepare MIPs including covalent, semi-covalent, non-covalent, metal ions mediated, and non-polar interaction (14). Each of these methods has its own advantages and disadvantages. In covalent method, less non-specific recognition sites are formed and a wider range of polymerization conditions is tolerable; however, a chemical modification should be done on template before and after MIP preparation. Non-covalent strategy is attractive because of its simplicity and its potential to cover a wide range of chemical functionalities. Moreover, non-covalent method form more stable cavity to maintain conformational structure in the absence of the template and impose more flexibility to the structure of polymer for ease of template realization and establishing fast equilibrium between the release and re-uptake of the template (15). However, this method has its own drawbacks such as heterogeneity of recognition sites, more number of non-specific binding sites and low yield of receptor sites with high affinity.

Olanzapine, as an example of new generation antipsychotics, has been considered as first line therapeutic for treatment of schizophrenia. Schizophrenia is a mental disorder in which the patient cannot think properly and has poor response to emotions. It is characterized by auditory hallucinations, paranoid or bizarre delusions, or disorganized speech and thinking, and it is accompanied by significant social or occupational dysfunction (16). Both genetic and environmental factors, such as premature birth, low birth weight, and prenatal hypoxia, social isolation, migrant status, and urban life, are important in development of symptoms of the disorder (17). Dopamine D2 receptor antagonists have been used to treat this disorder for years as first generation drugs. Due to the side effects of these drugs, the second generation drugs such as olanzapine has been developed in the recent decade.

Usually, elderly patients who suffer from schizophrenia and use olanzapine as long-term therapy may also have other diseases and disorders and should use several medications at the same time. The lesser the number of times a patient has to take different medicines per day the better he or she will follow the treatment with more compliance (18). Therefore, controlled release formulations are considered in this regard. Different techniques have been employed for controlling the drug release from a formulation which can govern the release process by various types of mechanisms such as diffusion, dissolution, osmosis, swelling, chemical interactions, hydrodynamic pressure, pH, and so on (19). Molecular imprinting is a type of chemical interaction which has recently been considered as a tool for drug delivery.

In this research work, an MIP system was synthesized and characterized employing non-covalent strategy using olanzapine as template, methacrylic acid (MA) as monomer, and ethylene glycol dimethacrylate (EGDMA) as a cross-linker in different solvent systems as porogen to study the morphology, loading efficacy, selectivity, *in vitro* release and *in vivo* controlled release efficacy of drug molecule.

MATERIALS AND METHODS

Materials

Olanzapine and clozapine were received as a gift from Aboureyhan Pharmaceutical Company, Tehran-Iran. Methacrylic acid (MA), ethylene glycol dimethacrylate (EGDMA), 2,2-azobis (2-isobutyronitrile) (AIBN), acetonitrile, methanol, ethanol, acetone, hydrochloric acid, chloroform, glacial acetic acid, ethyl acetate, and ascorbic acid were purchased from Merck, Germany. Dialysis bag with molecular weight cut off (MWCO) 12,000 g/mol, heparin sodium, ketamine hydrochloride, and xylazine hydrochloride were purchased from Sigma-Aldrich, USA. MA was further purified by distillation while other reagents were used as received. Male Wistar rats (210 ± 20 g) were used for animal studies.

Methods

Preparation of MIP Nano-particles (MINPs)

Precipitation polymerization was used to synthesize MINPs. Through a preliminary screening, specified amounts of template, monomer and cross-linker (Table I) were placed in a 100-ml polymerization tube and dissolved in a 35 ml mixture of chloroform and acetonitrile as solvent system and mixed overnight. The tube was then purged with nitrogen to replace oxygen, 0.02% total weight of monomer and cross-linker of initiator was added, sealed, and kept for 22 h in a water bath at a temperature of 60°C with continuous stirring. At the end of the polymerization, the solvent system was evaporated under vacuum and the product was washed several times with a mixture of methanol to acetic acid (9:1) for 1 h until no template remained within the polymer structure (the UV absorption of the supernatant at 252 nm was no longer observed). The resulting powder was then washed twice by purified water and once with acetone and was left to dry at room temperature. Similar steps were performed without using template to obtain non-MINPs.

Characterization of MINPs

Ultraviolet Spectroscopy. Drug concentration measurements for control of effective template removal after washing polymer system, loading experiments and selectivity were performed by ultraviolet spectroscopy (UV) spectroscopy using a UV/VIS spectrophotometer at 252 and 220 nm for olanzapine and clozapine, respectively (Optizem 2120 UV PLUS, Korea).

Fourier Transform Infra Red Spectroscopy (FT-IR). FT-IR spectrum of MINP-32 and non-MINP-32 was obtained in solid state (KBr as filler), at room temperature in the range

Table I. Mole Ratio of Template: Monomer: Cross-Linker, and Mixture of System Solvents Used to Prepare the MIP Nano-particles

Run numbers	Template (mmol)	MA (mmol)	EGDM (mmol)	$CHCl_3$ (%)	AcCN (%)	Reaction product
1	1	2	16	100	0	Rigid mass
2	1	2	16	85	15	Low level of fine particles
3	1	2	16	50	50	Low level of fine particles
4	1	2	32	100	0	Rigid mass
5	1	2	32	85	15	Low level of fine particles
6	1	2	32	50	50	Low level of fine particles
7	1	2	64	100	0	Rigid mass
8	1	2	64	85	15	Low level of fine particles
9	1	2	64	50	50	Low level of fine particles
10	1	4	16	100	0	Rigid mass
11	1	4	16	85	15	High level of fine particles
12	1	4	16	50	50	Low level of fine particles
13	1	4	32	100	0	Rigid mass
14	1	4	32	85	15	High level of fine particles
15	1	4	32	50	50	Low level of fine particles
16	1	4	64	100	0	Rigid mass
17	1	4	64	85	15	High level of fine particles
18	1	4	64	50	50	Low level of fine particles
19	1	6	16	100	0	Rigid mass
20	1	6	16	85	15	High level of fine particles
21	1	6	16	50	50	Low level of fine particles
22	1	6	32	100	0	Rigid mass
23	1	6	32	85	15	High level of fine particles
24	1	6	32	50	50	Low level of fine particles
25	1	6	64	100	0	Rigid mass
26	1	6	64	85	15	High level of fine particles
27	1	6	64	50	50	Low level of fine particles
28	1	8	16	100	0	Rigid mass
29	1	8	16	85	15	High level of fine particles
30	1	8	16	50	50	Low level of fine particles
31	1	8	32	100	0	Rigid mass
32	1	8	32	85	15	High level of fine particles
33	1	8	32	50	50	Low level of fine particles
34	1	8	64	100	0	Rigid mass
35	1	8	64	85	15	High level of fine particles
36	1	8	64	50	50	Low level of fine particles

4000–400 cm^{-1} using Nicolet FT-IR Magna 550 spectrophotometer (Thermo Electron Corporation, USA).

Thermal Gravimetric Analysis. Thermal gravimetric analysis (TGA) was used to assess the effect of structural configuration due to memorization of template inside the polymer backbone and justification of molecular imprinting employing Perkin Elmer Pyris Diamond TG/DTA analyzer (PerkinElmer Life and Analytical Sciences, USA). The temperature range was set from 25 to 700°C with increments of 20°C per minute under N2 gas.

Size and Zeta Potential. The size and poly-dispersity of MINP-32 was measured by photon correlation spectroscopy using a Zetasizer 3000HS (Malvern Instruments, Malvern, United Kingdom). The sample was diluted by filtered purified water and scattering angle was set at 90° for measurement. The measurement was done three times at 25°C and the mean values ± SD were reported.

The charge of the MINP-32 was measured by laser Doppler anemometry using a Zetasizer 3000HS (Malvern Instruments, Malvern, United Kingdom). The sample was diluted by filtered purified water which then placed in the electrophoretic cell, where a potential of 150 mV was established. The mean of at least 3 runs was used to be reported.

Scanning Electron Microscopy. The morphology of the MINP-32 and non-MINP-32 were assessed by scanning electron microscopy (SEM) (Philips XL30 scanning microscope, Philips, the Netherlands). An aqueous suspension of the particles was fixed, dried, and coated with gold. This operation in DC-magnetron sputtering was carried out for 10 min in DC plasma condition using Argon gas with DC voltage of 6 kV and DC current of 6 mA. The accelerator voltage for scanning was 20 kV (Vacc = 20 kV). Diameter of particles was determined using CLEMEX® particle image analysis software package.

Adsorption-Desorption Isotherm. Porosity and surface morphology of the MINP-32 were studied by measuring liquid N2 adsorption-desorption isotherm in a microporosimeter (BELSORP Mini, Japan). One hundred fifty milligrams of sample was dried in vacuo at 100°C for 3 h before analysis. Analysis was performed at 77K (−196°C). The specific surface

area was measured using the Brunauer-Emmett-Teller (BET) methodology. The specific pore volume and average pore diameter were calculated employing Barrett, Joyner, and Halenda (BJH) method.

Loading Experiments

Preliminary loading experiments were done as follows: 30 mg of washed MINPs and non- MIPNs were dispersed in 8 ml of a solution containing 250 μg/ml olanzapine in phosphate buffer to acetonitrile 4:1 (*v/v,* pH = 5.0) by sonication for 6 min and then stirred gently for 60 min. The liquid phase was then separated by centrifugation at 5000 rpm for 10 min and analyzed by UV at 252 nm (validated for quantitative analysis —data is not shown). The amount of drug bound to the polymers was calculated using the following equation:

$$Db(\%) = \frac{\mathrm{CA}-\mathrm{CB}}{\mathrm{CB}} \times 100$$

Where *Db* is the drug bound (loaded) to the polymers, CA is the initial drug concentration, and CB is the concentration of the drug in the liquid phase.

The MINP with maximum capacity of drug loading (MINPs-32, please refer to "RESULTS" and "DISCUSSION" and Fig. 2) was chosen and the optimum conditions for the loading were found by response surface methodology (RSM) using Box-Behnken methodology employing Design Expert 6.0.10 software (Stat-Ease, Inc., Minneapolis, USA). The effects of polymer (absorbent) amount, pH and time as the main factors were studied on drug loading as response. The lower and upper levels of the factors are chosen based on the results of preliminary studies which are as follows: 10 and 100 mg for polymer amount, 1 and 11 for pH, and 30 and 120 min for time. Experiment matrix design and responses are presented in Table II. Experimental runs were randomized to minimize the errors due to uncontrolled factors. Analysis of variance (ANOVA) was applied to investigate model fitness and effects of individual factors and their interactions on response. Based on RSM results, selectivity of MINP-32 was tested in comparison with its counterpart non-MINP by dispersing 79 mg of washed MINP-32 and non-MINP-32 in 30 ml solution containing 250 μg/ml olanzapine or clozapine at pH = 10.90, and stirred for 79 min at room temperature. The liquid phase was separated by centrifugation at 5000 rpm for 10 min and analyzed for free olanzapine and clozapine by UV spectroscopy at 252 and 220 nm, respectively (validated for quantitative analysis, data are not shown). The amount of loaded drug was calculated by the aforementioned formula.

Table II. Experimental Matrix Design for Binding Study with Results

Run	X_i	X_{ii}	X_{iii}	Y
1	55	11	120	89.0
2	55	11	30	58.0
3	10	11	75	39.0
4	55	6	75	31.0
5	10	1	75	2.0
6	55	1	30	0.5
7	55	6	75	29.0
8	100	6	30	35.0
9	10	6	30	16.0
10	55	1	120	40.0
11	10	6	120	13.0
12	55	6	75	19.0
13	55	6	75	33.0
14	100	11	75	98.0
15	55	6	75	30.0
16	100	6	120	47.0
17	100	1	75	15.0

X_i polymer amount (mg), X_{ii} pH, X_{iii} time (min), Y drug loading

In Vitro Study

Release Profile. Olanzapine was loaded on washed MINP-32 and non-MINP-32 as mentioned above. The precipitate after centrifugation was freeze dried and dispersed in 4 ml phosphate buffer saline (containing NaCl = 8 g, KCl = 0.2 g, Na2HPO4 = 1.44 g, KH2PO4 = 0.25 g in 1 l, adjusted at pH = 7.4) in a dialysis bag and floated in 16 ml of the same medium and shook at 37°C ± 0.5. One-milliliter samples were withdrawn at 0, 1, 2, 4, 8, 12, 24 h and, afterwards, once a day for 14 days with medium substitution to keep the sink condition. Drug release was determined by HPLC using KH2PO4 0.75 mMol, acetonitrile and methanol in a ratio of 55:40:5 adjusted at pH = 4.0 with orthophosphoric acid as mobile phase with a flow rate of 0.8 ml/min, a 250 mm × 4.6 mm, 10 μm C8 column [Lichrosorb RP-8 (10)], and UV detection at 227 nm. Injection volume was 20 μl.

Release Mechanism. The mechanism of drug release from MINP-32 was evaluated using common mathematical models. Among them, models with better fitting results (regression coefficients, $R_{\mathrm{sqr}} > 0.95$) were chosen for further analysis.

Higuchi model explains drug release from a matrix system mathematically which was first used for planar systems and then developed to different geometrics and porous systems. Drug release by diffusion according to Fick's law from a number of modified release pharmaceutical dosage forms is well described by this model (20). It relates the drug release to square root of time and is presented by the following equation (21):

$$\frac{Mt}{M\infty} = K_H t^{1/2}$$

in which $Mt/M\infty$ is the fractional drug release, K_H is the Higuchi constant and t is the time.

Korsmeyer and Peppas mathematical model simply relates time and release exponentially to each other to describe drug release from a polymeric system (22). This model has a strong ability to differentiate between different release mechanisms such as Fickian diffusion, Non-Fickian transport, case II (relaxation or swelling controlled)

transport, and supper case II (erosion controlled) transport. The model is presented as follows:

$$\frac{Mt}{M\infty} = K_p t^n$$

in which $Mt/M\infty$ is the fractional drug release, K_p is the model constant, t is the time, and n is the release exponent which its value characterizes the release mechanism.

Baker and Lonsdale mathematical model has been developed from the Higuchi model to explain the drug release from spherical matrices such as microcapsules or microspheres (20) according to the equation:

$$\frac{3}{2}\left[1-\left(1-\frac{Mt}{M\infty}\right)^{\frac{2}{3}}\right]\frac{Mt}{M\infty} = k1$$

in which $Mt/M\infty$ is the fractional drug release and $k1$ is the release rate constant.

Thermal Stability Study of the MINP-32. A suitable amount (about 450 mg) of MINP-32 was placed in a small beaker and kept at 50 ± 2°C/90 ± 5 relative humidity (RH) for one month. The assay and impurity profile of olanzapine was measured at the beginning, after 15 and 30 days of the study by HPLC method as described under "2.2.4.1 Release profile."

In Vivo Study of MINPs in Rat

All animal studies were performed in compliance with "The Basis of Laboratory Animal Science" prepared and published by Royan institute, 2013, ISBN: 978-600-92587-8-9. Twelve male Wistar rats (average body weight 210 ± 20 g) were divided in two groups of 6. A dispersion of MINP-32 containing 5 mg/Kg olanzapine in water for injection (after sonication for 24 h) was injected intramuscularly (IM) to the left leg of the animals in one group (test) and 5 mg/Kg olanzapine alone was injected in the same way to the other group (control). The animals were anesthetized using ketamine (50 mg/kg body weight) and xylazine (5 mg/kg body weight). After the onset of anesthesia (about 10 min) 1 ml blood samples were withdrawn directly from the heart of the fully anesthetized animals within 30 min at the beginning and then 24, 96, 168 and 240 h after injection.

Drug extraction was performed immediately after each sampling as follows: blood samples were transferred to heparinized tubes and centrifuged at 4000 rpm for 20 min. The supernatant liquid was transferred to another micro-tube and 1 ml ethyl acetate was added and vortexed for 1 min and centrifuged at 5000 rpm for 20 min. The upper liquid evaporated at 60°C under vacuum and stored at −80°C until analysis. Analysis was performed by HPLC with the same method aforementioned by dissolving the samples in 1 ml of mobile phase.

Statistical Analysis

All data is presented as mean ± standard deviation from three independent experiments. Statistical significant differences were assessed employing SPSS 11.5 software, using the Student t test with probability values < 0.05 assumed significant.

RESULTS

MINPs Formation and Characterization

The synthesis of the MINPs is schematically illustrated in Fig. 1. Non-covalent strategy was selected due to its benefits as aforementioned in the introduction. Different ratios of monomer and cross-linker against a fix amount of template as well as different solvents alone or in a mixture were examined to prepare the MINPs as presented in Table I. The preliminary criterion of selection was formation of MINPs as a fine powder directly in reaction mixture. Reaction in acetonitrile alone did not result in any polymer while a rigid mass resulted in chloroform alone. Therefore, only the product of reaction runs resulted in high level of fine particles were selected for binding experiments. The loading efficacy of the selected MINPs and counterpart non-MINPs was measured and the results are shown in Fig. 2. As can be seen in Fig. 2, MINP obtained from run number 32 shows the highest drug loading in comparison with its counterpart non-MINP and hence it was selected for further characterization, *in vitro* and *in vivo* studies.

Figure 3 shows the FT-IR spectrum of unwashed and washed MINP-32 (Fig. 3a, b) and non-MINP-32 (Fig. 3c). As can be expected, OH stretching vibration of non-MINP and MINP-32 (washed) are strong at 3438.4 cm^{-1} and 3434.4 cm^{-1}, respectively, whereas the OH vibration in MINP-32 (unwashed) has become weaker and transferred a little to the right (3431.6 cm^{-1}).

TGA thermogram of unwashed and washed MINP-32 and non-MINP-32 are presented in Fig. 4. Non-MINP-32 started to decompose at a lower temperature (about 280°C, Fig. 4d) than unwashed and washed MINP-32 (about 331–332°C, Fig. 4b, c). Olanzapine began to decompose at a temperature far below the temperature of polymer (about 220°C, Fig. 4a).

Morphology of nano-particles obtained by SEM is illustrated in Fig. 5. The size of non-MINP-32 (Fig. 5a) is significantly bigger than washed and unwashed MINP-32 (279 nm *versus* 117–122 nm, Fig. 5b, c) although there is no considerable difference in shape among them and all of them are almost spherical. These are almost in a good match with data obtained from size measurements obtained from photon correlation spectroscopy. The size for non-MINP-32 was measured 263 ± 5 nm and for washed and unwashed MINPs 123 ± 3 nm and 119 ± 4 nm, respectively, with a poly-dispersity index of 0.2 to 0.43. No significant difference was observed among Zeta potential of non-MINP-32, washed and unwashed MINP-32, and all was measured 6.9 ± 0.4 mV, 7.1 ± 0.2 mV, and 6.8 ± 0.4 mV, respectively.

According to the IUPAC classification (23), nitrogen adsorption-desorption isotherm of MINP-32 belongs to type IV isotherm which is an indication of a porous material

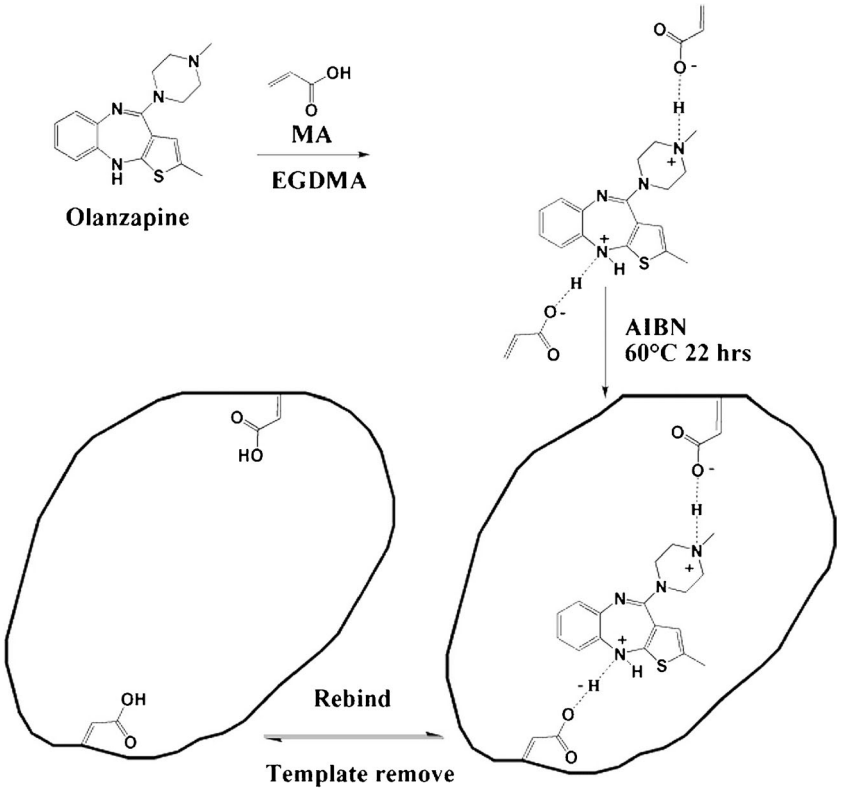

Fig. 1. Schematic illustration of MINPs synthesis

containing micropores (≤2 nm) and mesopores (2 to 50 nm). During adsorption phase, at lower pressure region, micropores filling occur until they are filled by a nitrogen monolayer completely. Then the mesopores continue to be filled by capillary condensation as the pressure increases. During desorption phase, as pressure is lowered, the mesopores are discharged by capillary evaporation. The capillary condensation and capillary evaporation do not take place at the same pressures, hence a hysteresis loop is created. MINP-32 shows a large specific surface area which is confirmed by type IV isotherm with a hysteresis loop at $P/P0 > 0.3$.

Optimization of Loading

To find optimum conditions for loading of template in its maximum possible amount, three independent factors in two levels were studied. Seventeen runs were performed to study response surface according to Box-Behnken methodology as

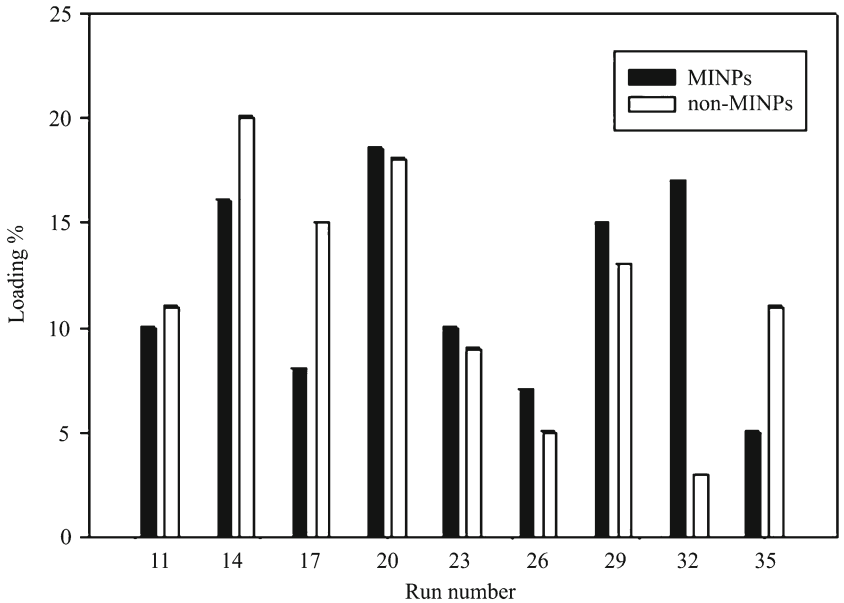

Fig. 2. Loading efficacy measurement of 9 MINPs and their counterpart non-MINPs (mean of 3 experiment ± SD)

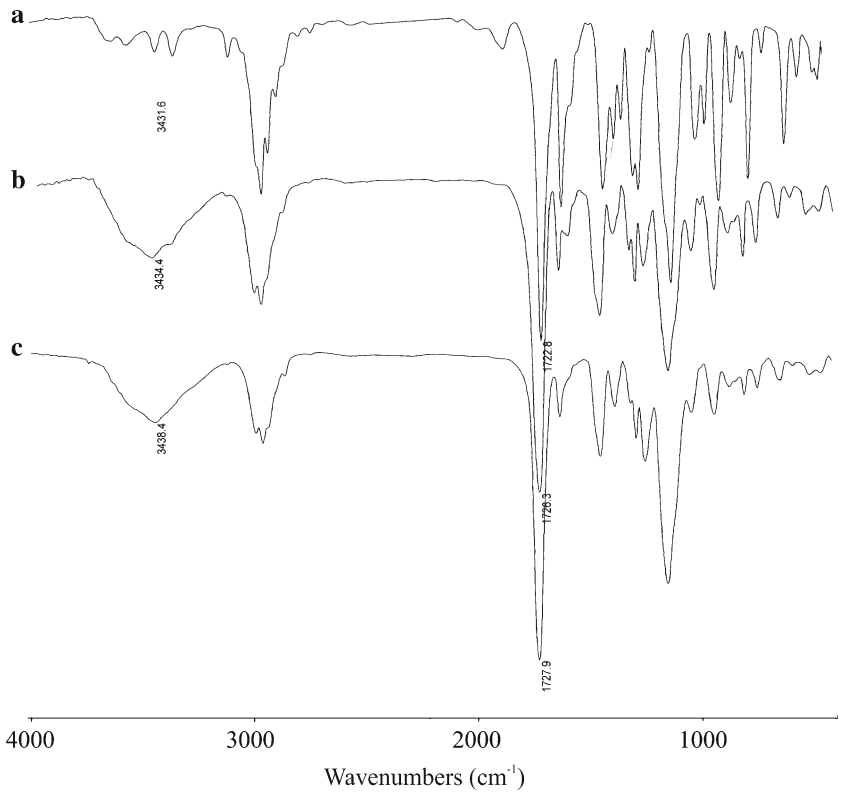

Fig. 3. FT-IR spectrums of unwashed MINP-32 (**a**), washed MINP-32 (**b**), and non-MINP-32 (**c**)

illustrated in Table II. Analysis of the data shows that the model is best fitted in quadratic model with a model *F* value of 26.6 which is significant. There is only a 0.01% chance that a large model *F* value like this could occur due to noise. Values of probability > *F* less than 0.05 were assumed significant for model terms and "not significant" terms were discarded. Among the model terms, pH has the highest effect on template loading with the highest *F* value. The "Lack of Fit *F* value" of 3.63 implies the lack of fit is not significant relative to the pure error. There is an 11.54% chance that a large lack of fit *F* value like this could occur due to noise. The value of 0.923612 for regression coefficient (*R*-Squared) shows that regression unable to explain only 7.6% of the total variability due to human or experimental errors. The predicted *R*-Squared of 0.7797 is in reasonable agreement with the adjusted *R*-Squared of 0.8889. Adequate precision measures the signal to noise ratio. A ratio greater than 4 is desirable. Our ratio of 18.034 indicates an adequate signal. This model can be used to navigate the design space.

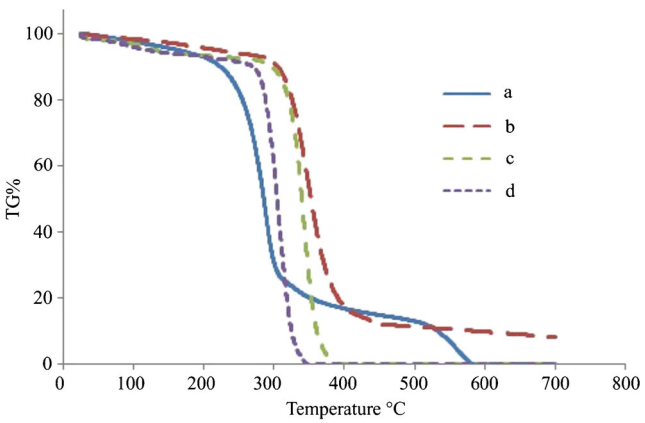

Fig. 4. TGA of olanzapine (**a**), unwashed MINP-32 (**b**), washed MINP-32 (**c**), and non-MINP-32 (**d**)

The effects of different factors on loading of template are illustrated in Fig. 6. As can be observed, pH has the maximum effect on loading, keeping time in its center value of 75 min. In lower pH, increasing the amount of absorbent does not show a significant increase in template loading. In contrast, in higher pH, by increasing the amount of absorbent the loading has also increased (Fig. 6b). In a fixed pH value at center point (pH = 6.0) by increasing the amounts of template and time, the loading has increased steadily (Fig. 6d). The effects of the template amount and time was not considerable at pH = 1.0, whereas at pH = 11.0, the effect of factors was considerable (data is not shown). In a fixed amount of template (center point), the effect of pH was more significant than time. The prominent effect of pH could be due to the physicochemical properties of template. Olanazapine is a weak base with a pK_a of 7.4 and is more soluble in acidic conditions; therefore, it is more ionized and cannot establish an effective interaction with polymer matrix. In contrast, in alkaline conditions the template molecule is less ionized and can interact with polymer matrix, probably through hydrogen binding as it is proved by FT-IR.

Based on data analysis the model equation can be written as follows:

$$Y = 0.040556X_i - 4.14528X_{ii} + 0.220833X_{iii} + 0.583056X_{ii}^2 + 0.051111X_iX_{ii} - 3.66694$$

Fig. 5. SEM of non-MINP-32 (**a**, ×18,000), unwashed MINP-32 (**b**, ×33,000), and washed template (**c**, ×21,000)

in which Y is loading, and X_i, X_{ii}, and X_{iii} are absorbent amount, pH, and time, respectively. In order to examine the validity of the model, three confirmation runs were performed according to the first suggested model solution for a loading of 85% within a range of 80–90% as lower and upper limits. Accordingly, 79 mg was used at pH = 10.90 with a mixture time of 79 min.

MINP-32 could have significantly distinguished between olanzapine and its analog clozapine in comparison with non-MINP-32. MINP-32 has absorbed about 85% of olanzapine and only 48% of clozapine, which imply almost a good selectivity of the polymer. In non-MINP-32, on the other hand, the ability of polymer to absorb olanzapine has decreased dramatically to 57% while for clozapine only to 42%.

In Vitro Study

Figure 7 presents the template release profile from MINP-32 and non MINP-32. Both drug loaded MINP-32 and non MINP-32 show a burst release of 32.5 and 59% in about 24 h, respectively. It could be due to the drug release from particles surface. The non MINP-32 releases almost all of its load (94%) and reaches to a plateau after 120 h while MINP-32 releases its load more slowly and reaches to its maximum release (95%) after 288 h.

Based on model fitting analysis for drug release from MINP-32, the release is best fitted in Korsmeyer and Peppas mathematical model with the highest regression coefficient R_{sqr} in comparison with other models (0.9837 *versus* 0.9786

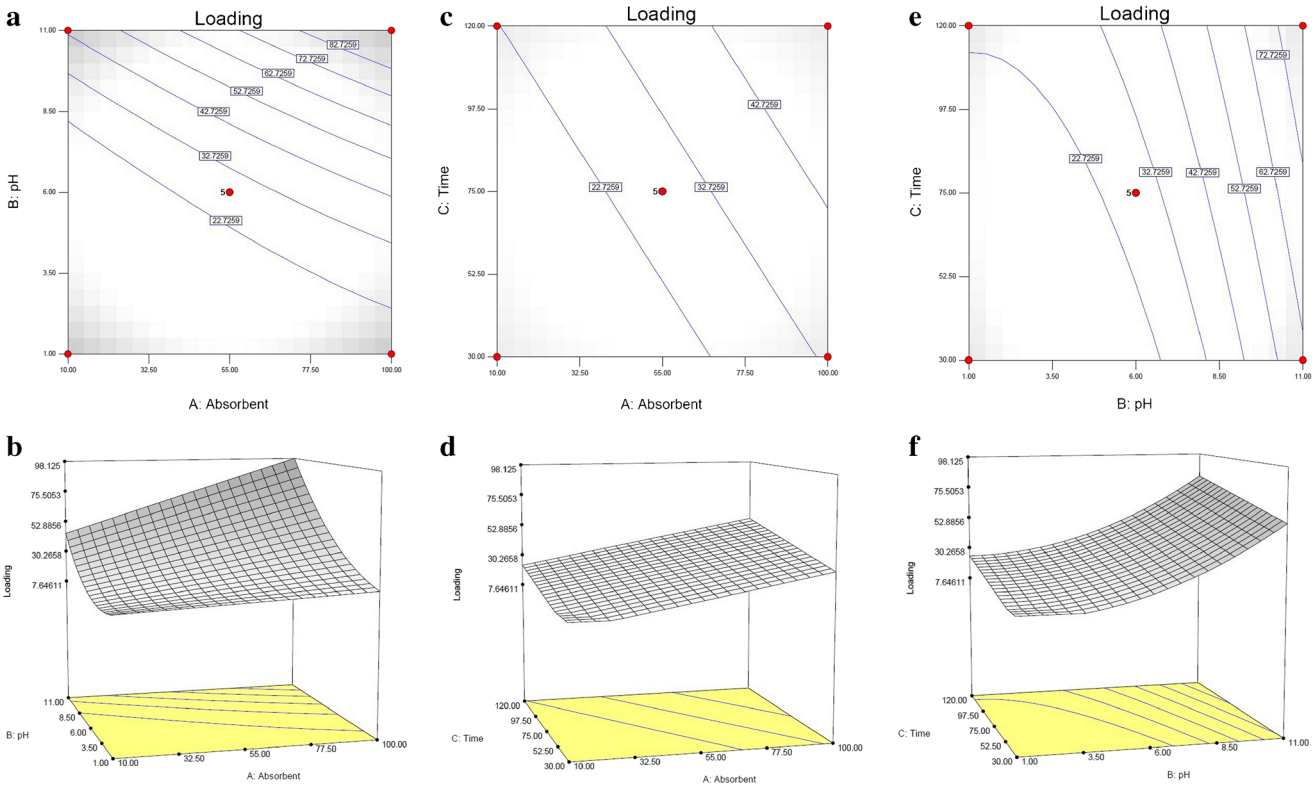

Fig. 6. Counter and three dimensional response surface plot of the effect of absorbent and pH (**a**, **b**), absorbent and time (**c**, **d**), and pH and time (**e**, **f**) on loading of template

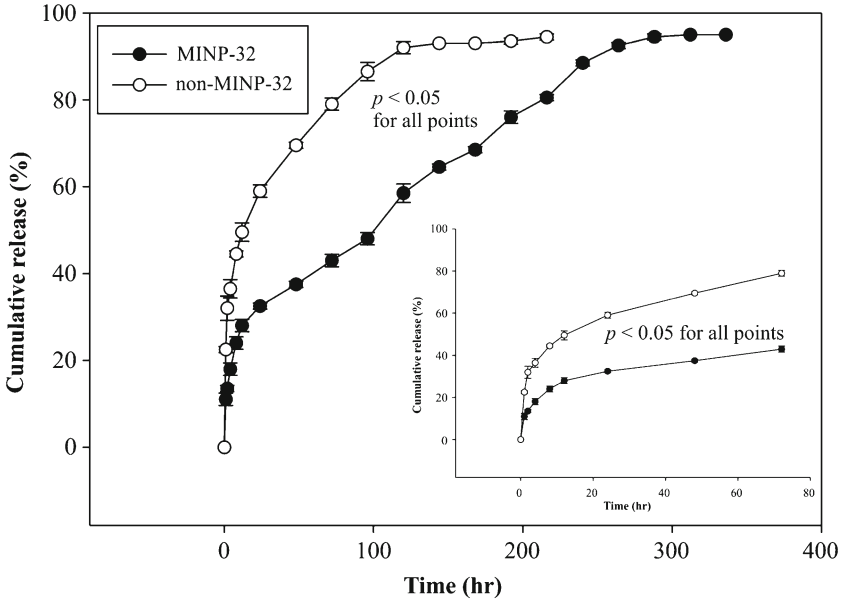

Fig. 7. Release profile of olanzapine from MINP-32 and non-MINP-32 (mean of 3 experiment ± SD) (Student's *t* test; $p < 0.05$ is significant)

for Higuchi model and 0.9681 for Baker and Lonsdale) and adjusted regression coefficient (Adj R_{sqr}) is in comply with R_{sqr}.

The amount of olanzapine in MINP-32 reduced not more than about 5% within one month kept at harsh condition of 50 ± 2°C/90 ± 5 RH compared to its initial amount before starting the study. An increase of less than 5% was measured in total impurities with observing no additional impurities after elapsing the stability condition.

In Vivo Study

Figure 8 demonstrates the plasma concentration of MINP-32 after IM administration. After 24 h, the serum concentration in the test group was measured 45–54 μg/ml in comparison to 90–100 μg/ml in control. These values after 72 h were 28–36 and 31–45 μg/ml, respectively. After 144 h, the plasma level in the test group decreased to 20–28 μg/ml while in control group it decreased to 5–10 μg/ml. After 216 h almost no drug was detectable in both test and control groups and therefore the experiments were terminated.

DISCUSSION

In FT-IR of MINP-32 (unwashed), OH vibration has become weaker and transferred a little to the right which could be due to hydrogen binding interaction between template and polymer matrix. The same phenomenon has observed and reported by others in the same polymeric system with the same composition but with different template (24). This is also confirmed by the TGA thermogram obtained from unwashed and washed MINP-32 and non-MINP-32. Polymeric matrix in MINP-32 has a more organized structure than non-MINP-32 and it is more robust than its non-MINP counterpart; therefore, it decomposes in higher temperatures than non-MINP.

As a result of interaction between template and polymer matrix it is expected that the size of MINP-32 particles would be smaller and that their shape would be more spherical than the non-MINP-32 particles. It is confirmed in size obtained from SEM as illustrated in "RESULTS" section. This could be due to synthesis method. To obtain homogenous and uniform nano-particles the reaction mixture was almost stirred vigorously throughout the whole reaction course in all runs. Therefore, there was no opportunity to have the primary particle cores formed in the beginning of the polymerization grown up and deviate from the spherical shape. In preliminary studies to set the polymerization conditions particles in micro scale with irregular shape were observed (data is not shown). In spite of olanzapine and polymer interaction, the stability of the template has not been affected by this interaction as can be seen from stability study. It confirms that there is no incompatibility between the template and polymer.

The MINP-32 has a very porous structure based on data obtained from nitrogen adsorption-desorption isotherm. With respect to the specific pore volume of 0.2315 cm3/g and average pore diameter of 3.1004 nm on the one hand and specific

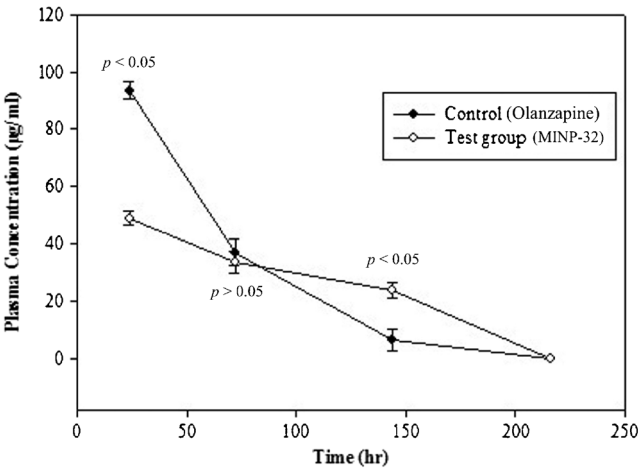

Fig. 8. Plasma concentration of olanzapine obtained from MINP-32 in comparison the olanzapine alone (mean of 3 experiment ± SD) (Student's *t* test; $p < 0.05$ is significant)

surface area of 298.64 m2/g on the other hand, a very porous structure is expected for MINP-32. Adsorption capacity of 150.4 mg/g confirms this expectation. The results are in good compliance with research works in this field (25,26).

The quadratic model used to optimize drug loading has a good power of prediction as examined for its validity. The amount of drug loading shows a maximum error of 3.55% which is acceptable. Therefore, it could be concluded that the quadratic model has a reasonable power of prediction within the experimental design range. The MINP-32 also showed a reasonable power of selectivity for its template in comparison with its analog.

The release profile of MINP-32 shows that it could have successfully kept the memory of the template and, hence, controlled the drug release due to effective weak interactions (*e.g.*, electro-static and hydrogen bound) between polymer functional groups and template (27). It is in good compliance with other research works reported by researchers who were interested to control the release of templates of their choice using the same polymeric system with the same composition (28–30). The mechanism of dug release is best fitted on Korsmeyer-Peppas model with exponent (n) value below 0.5 which reveals a quasi-Fickian transport from the NPs (31).

These results of animal study indicate that MINP-32 has the ability to control the release of its template. In test group, concentration of olanzapine decreases in a controlled manner within a longer time than control group. This data together with the release profile shows that MINP-32 has a desirable interaction with template to hold it for a long time and can be used as a controlled release drug delivery system for olanzapine.

CONCLUSION

In this research work MIMPs were synthesized for olanzapine as template. Based on our knowledge no research has yet been done in this field on olanzapine, and it is the first time a molecular imprinted system is made for this template. The results show that the developed MINP has a desirable memory of the template and has the ability to control the release. The selected MINP can also maintain its properties of keeping the memory of the template and controlling its release in biological environment.

Therefore, the MINPs of this research work could be a promising delivery system for olanzapine. Due to long-term *in vitro* release and *in vivo* plasma concentration profile of this delivery system it is expected that the system could be applied as intramuscular injection. More studies are under progress to assess toxicity properties of the system and its performance in long term stability studies, as well as its ability to be applied as subcutaneous injection or topical preparations such as dermal patches.

ACKNOWLEDGMENTS

We would like to acknowledge Dr. Abdollah Asadi [Department of Chemical Engineering, Amirkabir University of Technology (Tehran Polytechnic), Tehran, Iran] for his useful advices in synthesis of the MINPs and Niloofar Babanejad (Chemistry Department, Faculty of Sciences, IKIU, Qazvin, Iran) for her assistance in taking TGA thermograms and *in vitro* study. This research work was supported financially Tehran University of Medical Sciences (registration No. 89-03-33-11330).

COMPLIANCE WITH ETHICAL STANDARDS

Conflict of Interest The authors declare that they have no competing interests.

REFERENCES

1. Kim S, Kim JH, Jeon O, Kwon IC, Park K. Engineered polymers for advanced drug delivery. Eur J Pharm Biopharm Off J Arbeitsgemeinschaft Pharma Verfahrenstechnik eV. 2009;71(3):420–30.
2. Dinarvand R, Dorkoosh F, Hamidi M, Moghadam SH. Polymeric delivery systems for biopharmaceuticals. Biotechnol Genet Eng Rev. 2004;21(1):147–82.
3. Davis SS, Illum L, Stolnik S. Polymers in drug delivery. Curr Opin Colloid Interface Sci. 1996;1(5):660–6. English.
4. Pillai O, Panchagnula R. Polymers in drug delivery. Curr Opin Chem Biol. 2001;5:447–51. English.
5. Sellergren B, Allender CJ. Molecularly imprinted polymers: a bridge to advanced drug delivery. Adv Drug Deliv Rev. 2005;57(12):1733–41.
6. Takeuchi T, Haginaka J. Separation and sensing based on molecular recognition using molecularly imprinted polymers. J Chromatogr B. 1999;728:1–20. English.
7. Xu X, Zhu L, Chen L. Separation and screening of compounds of biological origin using molecularly imprinted polymers. J Chromatogr B Anal Technol Biomed Life Sci. 2004;804(1):61–9.
8. Ansell RJ, Kuah JK, Wang D, Jackson CE, Bartle KD, Clifford AA. Imprinted polymers for chiral resolution of (+/−)-ephedrine, 4: packed column supercritical fluid chromatography using molecularly imprinted chiral stationary phases. J Chromatogr A. 2012;1264:117–23.
9. Shi X, Wu A, Zheng S, Li R, Zhang D. Molecularly imprinted polymer microspheres for solid-phase extraction of chloramphenicol residues in foods. J Chromatogr B Anal Technol Biomed Life Sci. 2007;850(1–2):24–30.
10. Rathbone DL. Molecularly imprinted polymers in the drug discovery process. Adv Drug Deliv Rev. 2005;57(12):1854–74.
11. Sergeyeva TA, Slinchenko OA, Gorbach LA, Matyushov VF, Brovko OO, Piletsky SA, *et al.* Catalytic molecularly imprinted polymer membranes: development of the biomimetic sensor for phenols detection. Anal Chim Acta. 2010;659(1–2):274–9.
12. Cunliffe D, Kirby A, Alexander C. Molecularly imprinted drug delivery systems. Adv Drug Deliv Rev. 2005;57(12):1836–53.
13. Alvarez-Lorenzo C, Concheiro A. Smart drug delivery systems: from fundamentals to the clinic. Chem Commun (Camb). 2014;50(58):7743–65.
14. Mayes AG, Whitcombe MJ. Synthetic strategies for the generation of molecularly imprinted organic polymers. Adv Drug Deliv Rev. 2005;57(12):1742–78.
15. Vasapollo G, Sole RD, Mergola L, Lazzoi MR, Scardino A, Scorrano S, *et al.* Molecularly imprinted polymers: present and future prospective. Int J Mol Sci. 2011;12(9):5908–45.
16. Os JV, Kapur S. Schizophrenia. Lancet. 2009;374:635–45.
17. Picchioni MM, Murray RM. Schizophrenia. BMJ. 2007;335(7610):91–5.
18. Keith S. Advances in psychotropic formulations. Prog Neuro-Psychopharmacol Biol Psychiatry. 2006;30(6):996–1008.
19. Kumar S, Kumar A, Gupta V, Malodia K, Rakha P. Oral extended release drug delivery system a promising approach. Asian J Pharm Technol. 2012;2(2):38–43. English.
20. Dash S, Murthy PN, Nath L, Chowdhury P. Kinetic modeling on drug release from controlled drug delivery systems. Acta Pol Pharm Drug Res. 2010;67(3):217–23. English.
21. Higuchi T, Connors KA. Phase-solubility techniques. Adv Anal Chem Instrum. 1965;4:117–22. English.

22. Korsmyer RW, Gumy R, Doelker E, Buri P, Peppas NA. Mechanisms of solute release from porous hydrophilic polymers. Int J Pharm. 1983;15:25–35. English.
23. Sing KSW, Everett DH, Haul RAW, Moscou L, Pierotti RA, Rouquerol J, *et al*. Reporting physisorption data for gas-solid systems with specific reference to the determination of surface area and porosity. Pure Appl Chem. 1985;57(4):603–19. English.
24. Seifi M, Hassanpour Moghadam M, Hadizadeh F, Ali-Asgari S, Aboli J, Mohajeri SA. Preparation and study of tramadol imprinted micro-and nanoparticles by precipitation polymerization: microwave irradiation and conventional heating method. Int J Pharm. 2014;471(1–2):37–44.
25. Wei S, Molinelli A, Mizaikoff B. Molecularly imprinted micro and nanospheres for the selective recognition of 17beta-estradiol. Biosens Bioelectron. 2006;21(10):1943–51.
26. Chen J, Bai LY, Liu KF, Liu RQ, Zhang YP. Atrazine molecular imprinted polymers: comparative analysis by far-infrared and ultraviolet induced polymerization. Int J Mol Sci. 2014;15(1):574–87.
27. Lulinski P. Molecularly imprinted polymers as the future drug delivery devices.pdf. Acta Pol Pharm Drug Res. 2013;70(4):601–9. English.
28. Puoci F, Iemma F, Cirillo G, Picci N, Matricardi P, Alhaique F. Molecularly imprinted polymers for 5-fluorouracil release in biological fluids. Molecules. 2007;12:805–14. English.
29. Puoci F, Cirillo G, Curcio M, Iemma F, Parisi OI, Castiglione M, *et al*. Molecularly imprinted polymers for alpha-tocopherol delivery. Drug Deliv. 2008;15(4):253–8.
30. Cirillo G, Iemma F, Puoci F, Parisi OI, Curcio M, Spizzirri UG, *et al*. Imprinted hydrophilic nanospheres as drug delivery systems for 5-fluorouracil sustained release. J Drug Target. 2009;17(1):72–7.
31. El-Leithy ES, Shaker DS, Ghorab MK, Abdel-Rashid RS. Optimization and characterization of diclofenac sodium microspheres prepared by a modified coacervation method. Drug Discov Ther. 2010;4(3):208–16. English.